MEDICAL SCIENCE MONITOR

CLINICAL RESEARCH

e-ISSN 1643-3750
© Med Sci Monit, 2016; 22: 4177-4185
DOI: 10.12659/MSM.898546

Received: 2016.03.17
Accepted: 2016.04.24
Published: 2016.11.04

The Prevalence of Persistent Petrosquamosal Sinus and Other Temporal Bone Anatomical Variations on High-Resolution Temporal Bone Computed Tomography

Authors' Contribution:
Study Design A
Data Collection B
Statistical Analysis C
Data Interpretation D
Manuscript Preparation E
Literature Search F
Funds Collection G

ABCDEFG 1 **Paweł Bożek**
ABCDEFG 1 **Ewa Kluczewska**
ABCDEFG 2 **Maciej Misiołek**
ABCDEFG 2 **Wojciech Ścierski**
ABCDEFG 2 **Grażyna Lisowska**

1 Department of Radiology and Radiodiagnostics in Zabrze, Medical University of Silesia in Katowice, Zabrze, Poland
2 Department of Otorhinolaryngology and Laryngological Oncology in Zabrze, Medical University of Silesia in Katowice, Zabrze, Poland

Corresponding Author: Grażyna Lisowska, e-mail: grazyna.lisowska@onet.pl
Source of support: Self-financing

Background: The aim of the study was to determine the prevalence of petrosquamosal sinus (PSS) and other temporal bone (TB) anatomical variations in various patients using high-resolution computed tomography (CT).

Material/Methods: We reviewed clinical and consecutively obtained CT data for 276 TBs of 138 patients. The incidence of TB anatomical variations was compared among patients with radiological markers of chronic otitis media (RCOM) and non-RCOM.

Results: The PSS incidence in our sample was 6.9%, and it was significantly higher in TBs with RCOM (14.6%). Selected anatomical variations of RCOM TBs were observed: lateral sigmoid sinus (14.5%), prominent sigmoid sinus (23.6%), PSS (14.6%), and high jugular bulb (17.3%). Lateral sigmoid sinus and prominent sigmoid sinus ($p<0.01$), high jugular bulb ($p<0.05$), and PSS ($p<0.01$) were observed more often in RCOM than in non-RCOM TBs.

Conclusions: The TB vascular and anatomical variations, including PSS, a high jugular bulb, and a laterally and prominent placed sigmoid sinus, were more often observed in TBs with RCOM. Presurgical imaging and CT-based navigation techniques for TB surgery can offer remarkable value for understanding the altered anatomy of this complex structure and can localize rare anatomical variations.

MeSH Keywords: **Image Processing, Computer-Assisted • Models, Anatomic • Petrous Bone • Temporal Bone**

Full-text PDF: http://www.medscimonit.com/abstract/index/idArt/898546

2287 4 4 21

Indexed in: [Current Contents/Clinical Medicine] [SCI Expanded] [ISI Alerting System] [ISI Journals Master List] [Index Medicus/MEDLINE] [EMBASE/Excerpta Medica] [Chemical Abstracts/CAS] [Index Copernicus]

Background

Anatomic relationships in the temporal bone (TB) involve important vascular structures, including the sigmoid sinus, jugular bulb, and petrous segment of the internal carotid artery (ICA), closely associated nervous structures, inner ear structures, and pneumatized regions of TB. Numerous reports have detailed intraoperative middle ear surgery complications related to different TB anatomical variations [1,2]. Knowledge of those variations could be critical to avoid potential risk of intraoperative complications. We found a rare case of intraoperative complication due to profuse bleeding from the petrosquamosal sinus (PSS). In our clinical practice, PSS, high jugular bulb, and prominent sigmoid sinus were more frequently reported by radiologists in TBs with diploic or sclerotic mastoid and radiological evidence of chronic otitis media (RCOM). We decided to focus on this issue, owing to lack of published research on the incidence of anatomical variations in patients with decreased pneumatization of the mastoid or individuals with chronic otitis media (COM).

This study aimed to determine the prevalence of PSS, high jugular bulb, prominent sigmoid sinus, and laterally located sigmoid sinus on high-resolution computed tomography (CT) scan.

Material and Methods

We retrospectively analyzed 173 consecutive high-resolution CT examinations of the TB performed in two CT diagnostic centers, i.e., in our department and Voxel Medical Imaging Center, between 2011 and 2012. Available patient documentation and referrals were also analyzed with particular attention to CT indications and the clinical diagnosis or medical history of COM. In total, 138 CT exams of 276 TBs were included in the study. Among the 138 examined patients (mean age 54 years; range 8–90 years), 53% were women (n=71; mean age 54 years; range 15–86 years) and 47% were men (n=67; mean age 53 years; range 8–90 years). The clinically suspected diagnoses and symptoms that led to the CT examinations are described in Table 1.

Examined groups

The radiological data were independently reviewed and interpreted by one of two radiologists, who categorized TBs regarding RCOM. All TBs were divided into two groups: with radiological features of COM (n=110) and without radiological features of COM (n=166). The COM radiological criteria were observed in routine practice as follows [3]: sclerotic or diploic mastoid, presence of fibrous tissue in the neighborhood of the oval window with middle ear or mastoid effusion, thickness and/or retraction of the tympanic membrane, myringosclerosis, tympanosclerosis, destruction of the long process of the incus, destruction of the scutum, or cholesteatoma-like erosion of the bony borders of the middle ear or mastoid. If the TBs met two or more criteria listed above, they were included in the RCOM group. Three types of mastoid were distinguished: pneumatic, when pneumatization of mastoid air cells was full and complete; diploic, when pneumatization was partial; and sclerotic, when pneumatization was absent. In latter two categories, aeration was limited to an antrum and central mastoid tract of variable size. When the nonpneumatized portion of mastoid consisted of dense bone, it was categorized as sclerotic. Sclerotic or diploic mastoid was the main feature and was found in most cases (95.5%) in the RCOM group.

Inclusion criteria

The following inclusion criteria were used: age between 7 and 91 years, known medical history, and CT scan performed with the protocol described below.

Exclusion criteria

We excluded from the study the second and later exams of the same patient, exams that did not cover the entire analyzed anatomical region, and patients who had undergone severe surgical procedures of the examined region such that postsurgical changes did not allow assessment of the structures of interest.

Examination protocol

All of the TB CT examinations were performed using the same imaging protocol on the same type and model of scanner: General Electric LightSpeed 16 (GE Medical Systems, Milwaukee, Wisconsin, USA). Scans were obtained in helical mode, 120 kVp, and different mA currents depending on the patient anatomy and age. The minimal possible collimation was used. The native reconstruction algorithm was a 0.625-mm slice thickness with standard filtration and head scan field of view. The raw data from each TB were separated and reconstructed into axial images with a 0.625-mm slice thickness in the bone algorithm, with a an interval of 0.3 mm and a 100-mm display field of view to magnify small image details.

Post-processing and assessment

All TB CT scans were assessed using the Advantage Workstation (GE Healthcare, AW v. 4.5) and a multiplanar reformatting protocol in basic planes (sagittal, coronal, and axial). Axial images were standardized to be parallel to the lateral semicircular canal plane (Figure 1). Strict criteria for the analyzed structures, including TB vascular and anatomic variations, were defined (Table 2).

Indexed in: [Current Contents/Clinical Medicine] [SCI Expanded] [ISI Alerting System] [ISI Journals Master List] [Index Medicus/MEDLINE] [EMBASE/Excerpta Medica] [Chemical Abstracts/CAS] [Index Copernicus]

Table 1. Indication for CT examination (under referral) in all analyzed temporal bones (n=276) and in groups of temporal bones with radiological features of chronic otitis media (n=110).

Clinical indication for CT	All TBs n (%)	RCOM n (%)	p-value
Chronic otitis media	94 (34.1%)	84 (76.4%)	p<0.001
Suspicion of cholesteatoma	33 (11.9%)	31 (28.2%)	p<0.001
One-sided Tinnitus	30 (10.9%)	3 (2.7%)	p<0.001*
Suspicion of CPA pathology	28 (10.1%)	2 (1.8%)	p<0.001*
Post-surgery TB assessment	18 (6.5%)	17 (15.5%)	p<0.001
One-side sensorineural hearing loss	24 (8.7%)	5 (4.6%)	
Vertigo	17 (6.2%)	13 (11.8%)	p<0.002
Ear injury/trauma	16 (5.8%)	2 (1.8%)	p<0.05*
Hearing loss (undefined)	15 (5.4%)	2 (1.8%)	p<0.05*
Headache	10 (3.6%)	6 (5.5%)	
Conductive hearing loss	8 (2.9%)	2 (1.8%)	
External auditory canal pathology	8 (2.9%)	2 (1.8%)	
Otosclerosis	6 (2.2%)	0 (0%)	
Pain in the ear	5 (1.81%)	1 (0.9%)	
Prior cochlear implantation assessment	2 (0.72%)	0 (0%)	
Tumor suspicion	2 (0.72%)	0 (0%)	
Assessment of stapes prosthesis	1 (0.36%)	0 (0%)	
Tympanic membrane perforation	1 (0.36%)	0 (0%)	
Other reason for examination	3 (1.08%)	1 (0.9%)	

* Negative relationship: the incidence among those indicated for CT was significantly lower in the group of RCOM TBs than TBs with no radiological signs of COM; TB – temporal bone; COM – chronic otitis media; RCOM – temporal bones with radiological features of chronic otitis media; CPA – cerebellopontine angle.

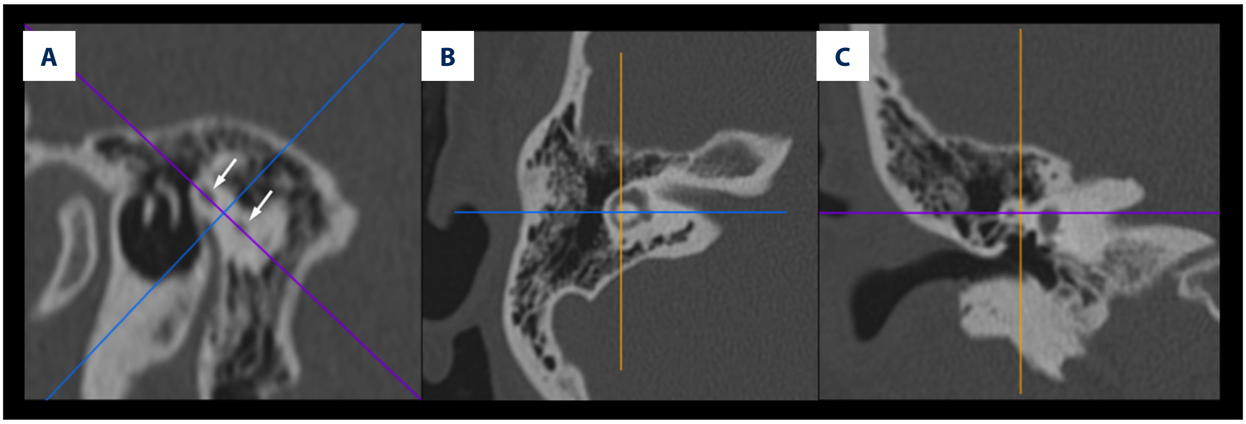

Figure 1. Standardization of the axial plane (**B**) using the "two-dots" technique in multiplanar reformatting reconstruction of computed tomography data. After identification of the lateral semicircular canal in the sagittal plane (**A**), an axial cross-reference line (purple line) was drawn through two dots (arrows) that represent the anterior and posterior branches of the lateral semicircular canal. Perpendicular to the axial line, other reconstruction plane cross-reference lines are shown: a blue line for the coronal plane (**C**) and a yellow line for the sagittal plane (**A**).

Indexed in: [Current Contents/Clinical Medicine] [SCI Expanded] [ISI Alerting System] [ISI Journals Master List] [Index Medicus/MEDLINE] [EMBASE/Excerpta Medica] [Chemical Abstracts/CAS] [Index Copernicus]

Table 2. Analyzed vascular and anatomic variations.

Structure	Abbreviation	Imaging criteria
High jugular bulb	HJB	Highest point of the jugular bulb is over the plane of the bottom portion of the internal auditory canal on standardized axial images; perpendicular to the plane of the lateral semicircular canal
Prominent jugular bulb	Pro-JB	Significantly larger jugular bulb compared to the opposite side
Dehiscent jugular bulb	DJB	Absence of hyperdense bony septa between tympanic cavity and jugular bulb (not caused by COM or surgery)
Jugular bulb diverticulum	JBD	Isolated finger-like projection extending from the jugular bulb into the surrounding bone
Dehiscent facial nerve canal	DCN7	Dehiscent mastoid segment of the facial nerve bony canal by a prominent or high jugular bulb
Lateralized or dehiscent internal carotid artery	Lat-ICA	Dehiscent bony wall of petrous ICA with or without artery protrusion into the middle ear
Aberrant internal carotid artery	Ab-ICA	Displaced ICA running through the middle ear
Persistent stapedial artery	PSA	Foramen spinosum is absent, and an artery running parallel to the promontorium through stapes footplate is present
Prominent sigmoid sinus	Pro-SS	Prominent sigmoid sinus compared to the opposite side
Laterally located sigmoid sinus	Lat-SS	Protrusive type of sigmoid sinus [6] placed laterally, with a reduced distance between the sigmoid sinus and mastoid cortex
Anteriorly located sigmoid sinus	Ant-SS	Protrusive type of sigmoid sinus [6] placed anteriorly, with a reduced distance between Henle's spine and the sigmoid sinus
Petrosquamosal sinus	PSS	Occurrence and diameter of petrosquamosal sinus; aberrant vascular channel in the bony canal in the mastoid roof draining to the sigmoid sinus running in an anterio-posterior direction
Jugular bulb-vestibular aqueduct dehiscence	JBVAD	Dehiscence of vestibular aqueduct caused by jugular bulb

Statistical methods

All statistical calculations were performed using STATISTICA version 10.0 (StatSoft, Inc., 2011), R version 2.15.1, and Microsoft Excel. Student's t-test or the Mann-Whitney U test was used to test the significance of comparisons between two groups. Significant differences among more than two groups were evaluated using analysis of variance or the Kruskal-Wallis test. To test for independence, the chi-squared test (using the Yates correction for cell numbers <10) or Fisher's exact test was used for categorical variables. Pearson's and/or Spearman's correlation coefficient was used to establish relationships and their strength and direction between the variables. P<0.05 was considered significant.

Results

The incidence of TB vascular and anatomical variations is presented in Table 3. No persistent stapedial artery or aberrant ICA was observed. Only one patient (2 TBs, <1%) had a bilateral abnormal vascular channel in the petrous part of the TB, which connects the sigmoid sinus and the superior petrosal sinus and may therefore correspond to a persistent lateral capital vein as previously described [1] (Table 3). Other analyzed structures also differed among the studied groups (Table 3).

In TBs with RCOM (n=110), sclerotic mastoid was found in 52.7% (n=58), diploic mastoid was found in 41.8% (n=46), and normal pneumatization of mastoid was present in 5.5% (n=6) of cases (p<0.01).

Relationships between the incidence of TB anatomical variations and RCOM are presented in Table 4. High jugular bulb (p<0.05), dehiscence of the mastoid portion of the bony facial nerve canal (p<0.05), PSS (p<0.01), laterally located sigmoid sinus (p<0.01), and prominent sigmoid sinus (p<0.01) were more frequently observed in RCOM TBs than in non-RCOM TBs (Table 4). Other anatomical and vascular abnormalities did not differ between groups.

The diameter of the PSS bony canal significantly differed between RCOM and non-RCOM TBs (p<0.01). The mean bony canal diameter of the PSS in all TBs was 1.1 mm (range 0.7–3.4 mm).

Indexed in: [Current Contents/Clinical Medicine] [SCI Expanded] [ISI Alerting System] [ISI Journals Master List] [Index Medicus/MEDLINE] [EMBASE/Excerpta Medica] [Chemical Abstracts/CAS] [Index Copernicus]

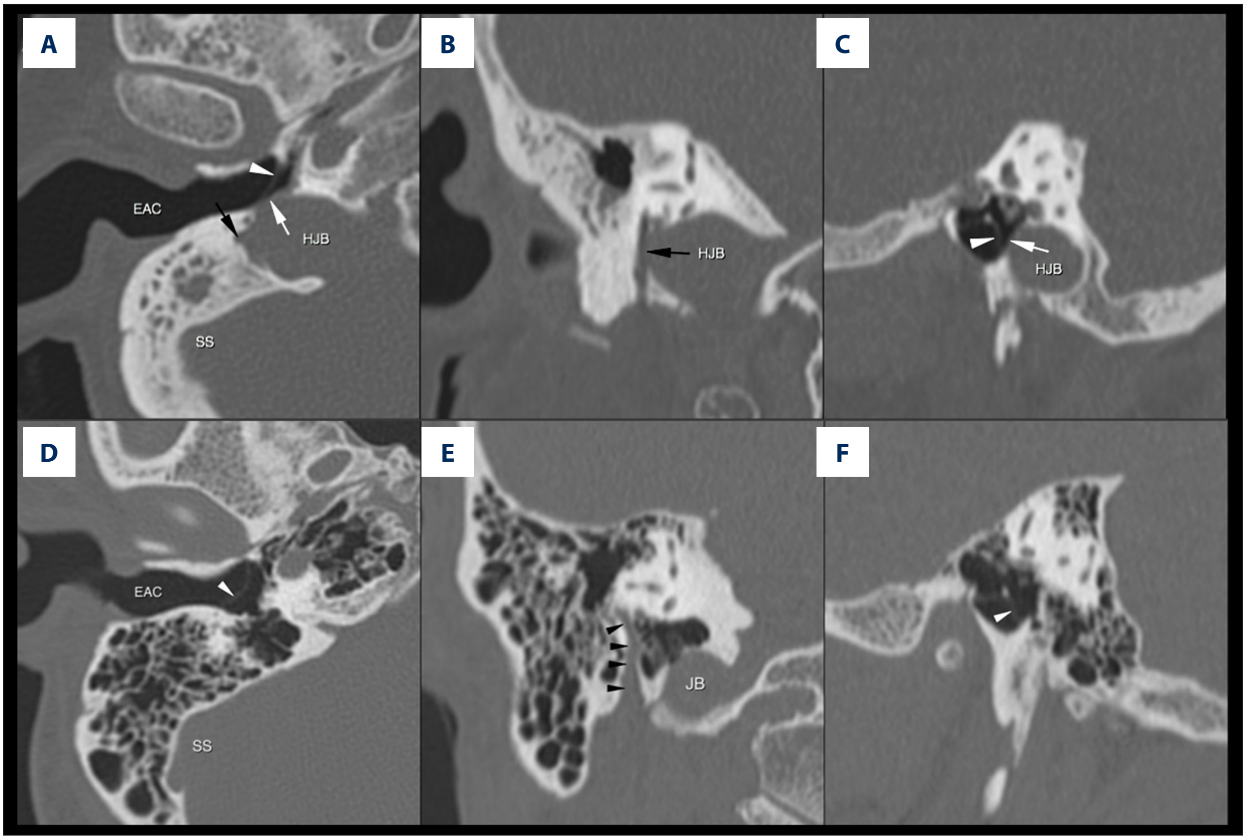

Figure 2. Multiplanar reformatting reconstructions of temporal bone computed tomography scan of a 52-year-old male with chronic otitis media and high jugular bulb (**A–C**) and of a normal jugular bulb of a 50-year-old male (**D–F**). Dehiscent high jugular bulb (white arrow) and dehiscent mastoid portion of the facial nerve canal (black arrow) caused by a prominent and high jugular bulb can be best seen in the coronal plane (**B**). In the axial (**A**) and sagittal (**C**) planes, the tympanic membrane can be seen (white arrowhead), and it is very close to the jugular bulb. Diploic mastoid, normal external auditory canal, and normal location of the sigmoid sinus are shown in the axial plane (**A**). The normal appearance of the jugular bulb, mastoid, and mastoid portion of the facial nerve canal (black arrowheads) can be seen in the coronal plane (**E**). Normal pneumatization of the mastoid and location of the sigmoid sinus can be seen in the axial plane (**D**).

Jugular bulb-vestibular aqueduct dehiscence occurred more often in woman ($p<0.05$). No other strict association was observed between vascular or anatomical variations and patient age and sex. The highest contingency coefficient value for PSS was observed in RCOM TBs. A laterally located sigmoid sinus, prominent jugular bulb, jugular bulb-vestibular aqueduct dehiscence, and prominent sigmoid sinus occurred more often on the right side than the left ($p<0.01$).

Discussion

The anatomical variations of the TB could be the reason for many different serious intraoperative complications during ear surgery and neurosurgery procedures [4–7]. Recent data suggest that patients with venous pulsatile tinnitus may have multiple vascular anomalies or variants on the symptomatic side [8]. Furthermore some variations can be misinterpreted as pathological conditions and, as a result, contribute to further unnecessary diagnostic tests or examinations [9]. Our result shows that variants, including persistent PSS, a high jugular bulb, and a laterally or prominent placed sigmoid sinus, are more common in TBs with RCOM.

Different vascular variations, including a prominent jugular bulb with dehiscence of the bony margins (Figure 2), anteriorly located sigmoid sinus, or dehiscent ICA of the TB region, were reported to be a cause of intraoperative complications associated with profuse bleeding during surgery [2,6–8]. We observed one case with perioperative complications arising from profuse bleeding from a PSS that was considered by the surgeon to have been caused by damage to the anteriorly located sigmoid sinus (Figure 3). We found no cases of such PSS-related intraoperative complications in the literature. However, Choi and Woo described one case of this anomaly correctly diagnosed by preoperative imaging in a patient with COM in whom PSS coexisted with a laterally placed sigmoid sinus [10], and An et al. described two cases of PSS as a perioperative finding

Indexed in: [Current Contents/Clinical Medicine] [SCI Expanded] [ISI Alerting System] [ISI Journals Master List] [Index Medicus/MEDLINE] [EMBASE/Excerpta Medica] [Chemical Abstracts/CAS] [Index Copernicus]

Table 3. Incidence of temporal bone anatomical variations in the studied groups: all temporal bones (n=276), temporal bones with radiological features of COM (RCOM) (n=110) and type of mastoid.

Structure	All TBs	RCOM	Sclerotic mastoid	Diploic mastoid	Pneumatic mastoid
No. of TBs (n)	276	110	60	68	148
HJB	33 (11.96%)	19 (17.27%)	14 (23.33%)	8 (11.76%)	11 (7.43%)
Pro-JB	37 (13.41%)	20 (18.18%)	14 (23.33%)	5 (7.35%)	18 (12.16%)
DJB	5 (1.81%)	3 (2.73%)	2 (3.33%)	1 (1.47%)	2 (1.35%)
JBD	11 (4%)	6 (5.45%)	5 (8.33%)	1 (1.47%)	5 (3.4%)
DCN7	4 (1.45%)	4 (3.64%)	3 (5%)	1 (1.47%)	0 (0%)
Lat-ICA	9 (3.36%)	5 (4.55%)	4 (6.67%)	1 (1.47%)	4 (2.7%)
Pro-SS	43 (15.58%)	26 (23.64%)	14 (23.33%)	9 (13.24%)	20 (13.51%)
Lat-SS	23 (8.33%)	16 (14.55%)	8 (13.33%)	11 (16.18%)	4 (2.7%)
Ant-SS	3 (1.09%)	2 (1.82%)	2 (3.33%)	0 (0%)	1 (0.68%)
PSS	19 (6.88%)	16 (14.55%)	8 (13.33%)	8 (11.76%)	3 (2.03%)
JBVAD	19 (6,88%)	10 (9,09%)	6 (10%)	5 (7.35%)	8 (5.41%)

RCOM – temporal bones with radiological features of chronic otitis media; HJB – high jugular bulb; Pro-JB – prominent jugular bulb; DJB – dehiscent jugular bulb; JBD – jugular bulb diverticulum; DCN7 – dehiscent facial nerve canal; Lat-ICA – lateralized or dehiscent internal carotid artery; Pro-SS – prominent sigmoid sinus, Lat-SS – laterally located sigmoid sinus; Ant-SS – anteriorly located sigmoid sinus; PSS – petrosquamosal sinus; LCV – lateral capital vein; JBVAD – jugular bulb-vestibular aqueduct dehiscence.

Table 4. Relationships between the incidence of temporal bone anatomical variations and temporal bones with radiological features of COM, side of anatomical variation and patient sex. Fisher's exact test was used for statistical analysis.

Parameter	Male	Female	p-value	Left TB	Right TB	p-value	RCOM=1	RCOM=0	p-value
No. of TBs (n)	134	142		138	138		110	166	
HJB	14 (10.4%)	19 (13.4%)		14 (10.1%)	19 (13.8%)		19 (17.3%)	14 (8.4%)	<0.05
Pro-JB	19 (14.2%)	18 (12.7%)		6 (4.4%)	31 (22.5%)	<0.01	20 (18.2%)	17 (10.2%)	
DCN7	2 (1.5%)	2 (1.4%)		0 (0.0%)	4 (2.9%)		4 (3.6%)	0 (0.0%)	<0.05
Pro-SS	19 (14.2%)	24 (16.9%)		7 (5.1%)	36 (26.1%)	<0.01	26 (23.6%)	17 (10.2%)	<0.01
Lat-SS	8 (6.0%)	15 (10.6%)		5 (3.6%)	18 (13.0%)	<0.01	16 (14.6%)	7 (4.2%)	<0.01
PSS	7 (5.2%)	12 (8.5%)		11 (8.0%)	8 (5.8%)		16 (14.6%)	3 (1.8%)	<0.01
JBVAD	4 (3.0%)	15 (10.6%)	<0.05	4 (2.9%)	15 (10.9%)	<0,01	10 (9.1%)	9 (5.4%)	

RCOM – temporal bones with radiological features of chronic otitis media; HJB – high jugular bulb; Pro-JB – prominent jugular bulb; DCN7 – dehiscent facial nerve canal; Pro-SS – prominent sigmoid sinus, Lat-SS – laterally located sigmoid sinus; PSS – petrosquamosal sinus; JBVAD – jugular bulb-vestibular aqueduct dehiscence.

in patients with COM [11]. The PSS incidence in our sample was 6.9%, and it was significantly higher in TBs with RCOM (14.6%). Koesling et al. [12] described a 1.4% incidence of this anomaly in routine TB CT examinations, which is lower than that in our sample. In contrast, PSS incidence is higher in anatomical studies and was observed in up to 23% of corrosion casts, as noted by San Millán Ruiz et al. [13]. We believe that this difference in radiological studies may have resulted from different data assessment techniques (axial *vs.* multiplanar reformats) and scanning protocols (higher resolution helical technique). In most of our cases, PSS was a small-diameter vessel only observed on coronal reformats of high-resolution data,

Indexed in: [Current Contents/Clinical Medicine] [SCI Expanded] [ISI Alerting System] [ISI Journals Master List] [Index Medicus/MEDLINE] [EMBASE/Excerpta Medica] [Chemical Abstracts/CAS] [Index Copernicus]

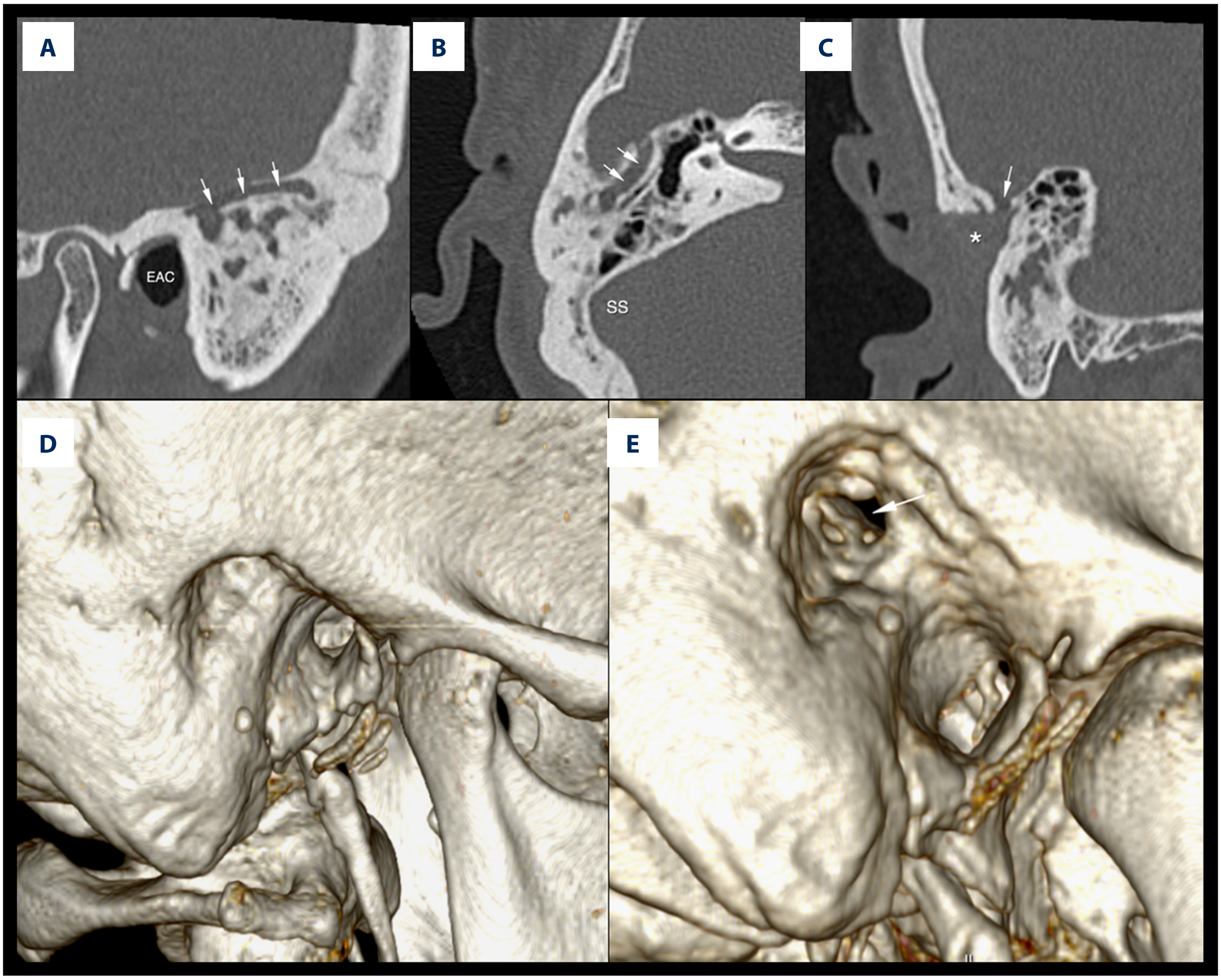

Figure 3. Multiplanar reformatting (**A–C**) and three-dimensional volume rendering (3D VR) (**D**) reconstructions of temporal bone computed tomography scan of a 53-year-old female with chronic otitis media after mastoidectomy (asterisk) of the right temporal bone. There was intraoperative profuse bleeding from a damaged petrosquamosal sinus (PSS; white arrows), which on referral was considered by the surgeon to have been caused by damage to the anteriorly located sigmoid sinus (SS). Normal location of the SS on axial scans (**B**) and postoperative changes of the mastoid (white asterisk) in the coronal plane (**C**) are shown. (**A**) Sagittal plane. (**B**) Axial plane. (**C**) Coronal plane. (**D**) 3D VR of the right mastoid; bony deficit after mastoidectomy is shown, with damage to the bony canal of the PSS.

and it was hard to localize on axial scans without performing multiplanar reformats. Koesling et al. did not analyze the PSS incidence in relation to RCOM and assessed only axial images. Giessmann et al. described a high (up to 65%) incidence of PSS in cochlear implant candidates with complete aplasia of the semicircular canals, which was higher than that observed in association with other inner ear malformations [14]. The mean diameter of PSS observed in our study (1.1 mm, range 0.7–3.4 mm) was smaller than that observed by Giessmann et al. (3.1 mm, range 1.0–4.4 mm) and San Millán Ruiz et al. (2.6 mm, range 2.0–3.0 mm) [13,14].

No simple explanation exists for the higher incidence of PSS in TBs with RCOM. PSS is generally believed to disappear early in embryonic life. However, in contrast to radiological images, PSS is not infrequently found in anatomical studies. Radiological identification of PSS usually relies on visualization of a bony canal within the temporal squama on CT scan (Figure 4) or groove of PSS over the TB; PSS can be found in a typical location on imaging studies, as described by Marsot-Dupuch et al. [15]. However, the proximity of PSS to the bone and its small size make its detection by CT, magnetic resonance imaging, or even digital subtraction angiography quite challenging, which in our opinion may explain the discrepancies in the prevalence of PSS documented during anatomical and imaging studies. Probably, in most cases PSS can be identified by imaging techniques only if persisting as a large channel or enclosed within a bony canal. The loss of mastoid volume and reduction of

Indexed in: [Current Contents/Clinical Medicine] [SCI Expanded] [ISI Alerting System] [ISI Journals Master List] [Index Medicus/MEDLINE] [EMBASE/Excerpta Medica] [Chemical Abstracts/CAS] [Index Copernicus]

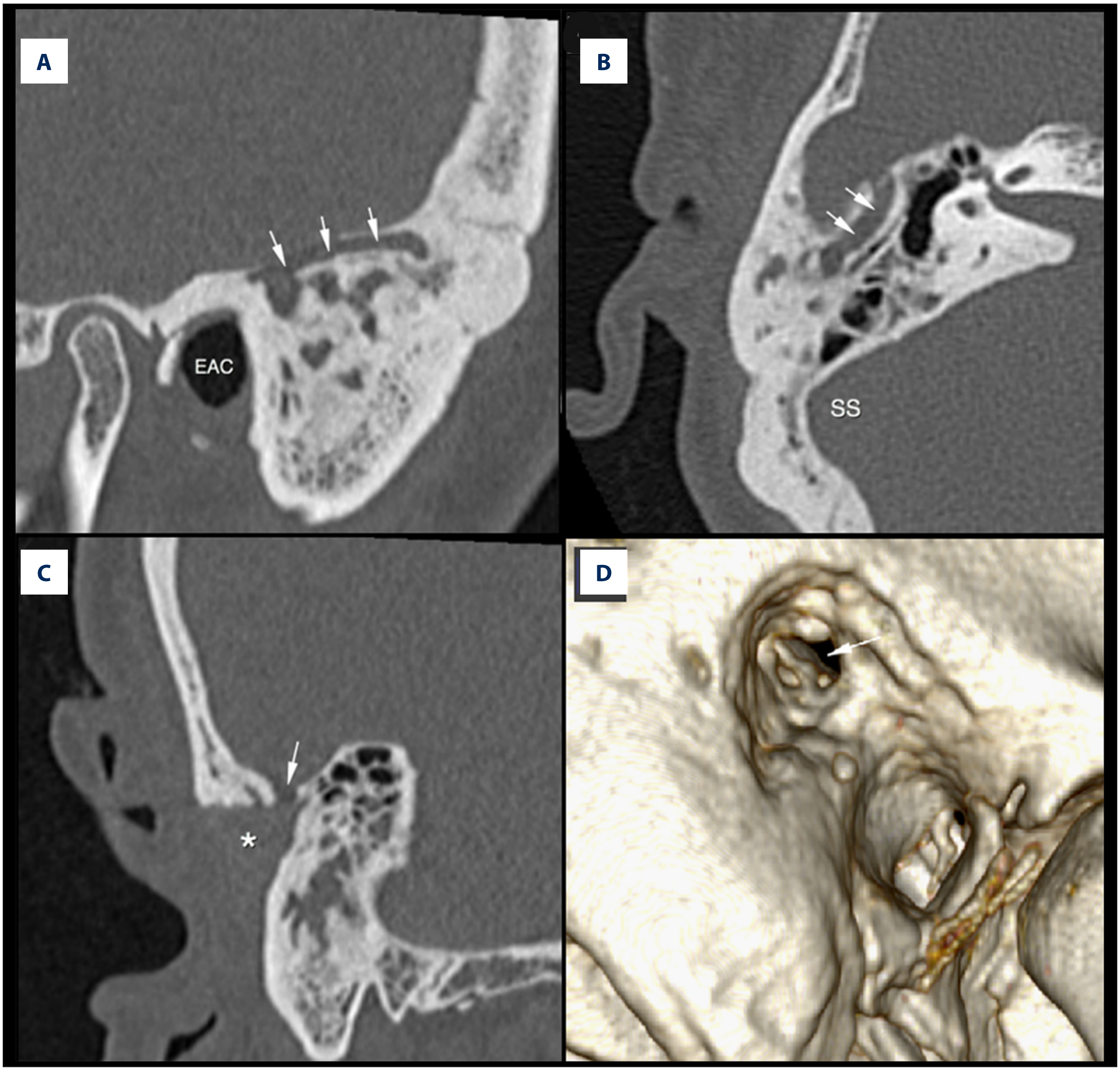

Figure 4. Multiplanar reformatting reconstructions of temporal bone computed tomography scan of a 38-year-old female with chronic otitis media and persistent petrosquamosal sinus (PSS) in the bony canal (white arrows). The axial plane (**A**) shows a sclerotic mastoid with a half-moon type of sigmoid sinus and a large PSS canal (white arrows). In the coronal plane (**B**), the bony deficit of the external auditory canal and mastoid after canal-wall-down surgery necessitated by cholesteatoma and a PSS bony canal (white arrow) are shown. In the sagittal plane (**C**), the PSS bony canal (white arrows) running through the anterior part of the temporal bone is shown.

the distance between middle fossa dura and external auditory canal in COM patients may improve visualization of the bony canal or changes in venous flow within this region. Due to inherent limitations of conventional CT, very small veins might have been either missed or remained beyond the capability of this technique. Detector collimation used in a standard TB CT scan ranges between 0.5 mm and 0.75 mm. Perhaps, detection of PSS and our knowledge in this matter could be improved by the use of cone-beam CT with resolution of less than 0.2 mm. We believe that the higher incidences of PSS, high jugular bulb, and lateral sigmoid sinus in TBs with the RCOM are related to sclerotization, reduction of mastoid size, and the distances from the sigmoid sinus and middle fossa dura to the external auditory canal or mastoid tip [16].

The overall incidence of dehiscence of the ICA bony covering (3.4%) was slightly higher than the 2% incidence observed by Koesling et al. [12] and the 1.4% incidence observed by

Indexed in: [Current Contents/Clinical Medicine] [SCI Expanded] [ISI Alerting System] [ISI Journals Master List] [Index Medicus/MEDLINE] [EMBASE/Excerpta Medica] [Chemical Abstracts/CAS] [Index Copernicus]

Atilla et al. [18], and lower than the 6.9% incidence observed by Wang et al. [17]. We analyzed CT scans acquired using a higher resolution technique than that used by Koesling et al. and Atilla et al., and a lower resolution than that used by Wang et al., which could explain the differences in the results [17]. Atilla et al. examined CT scans of 350 adult patients and excluded ears with evidence of COM, trauma, or tumor. The incidence of high jugular bulb ranged from 6% to 21.6% in CT studies [12,18,20] and was approximately 16% in one histological study [21]. By comparison, we observed a lower overall high jugular bulb incidence (12%). High jugular bulb criteria differ among studies, and a higher high-riding jugular bulb incidence has been reported when the high jugular bulb extends over the level of the round window, the inferior aspect of the bony annulus, and the basal turn of the cochlea, not above the bottom portion of the internal auditory canal, as in our study [17,18,21]. Moreover, most authors have excluded TBs with cholesteatoma or post-inflammatory changes observed on CT and analyzed structures in the axial plane without standardization, making the evaluation dependent on the patient's head position during acquisition of the scan [9,12,18,20]. The dehiscent jugular bulb incidence has been reported to range from 1% to 9.5%; no reports have investigated dehiscence of the mastoid portion of the facial canal caused by a prominent or high jugular bulb [9,12,18,20]. In contrast to other authors [17], we found no relationship between the coexistence of high jugular bulb and a dehiscent or aberrant ICA canal, perhaps because of the more strict high jugular bulb criteria and lower resolution CT technique in our study.

Conclusions

The TB vascular and anatomical variations, including PSS, a high jugular bulb, and a laterally or prominent placed sigmoid sinus, are more often observed in TBs with RCOM. Presurgical imaging and CT-based navigation techniques for TB surgery can offer remarkable value for understanding the altered anatomy of this complex structure and localize rare anatomical variations.

Disclaimers

No conflicts of interest are noted. No relationships with industry are noted.

References:

1. Hermans R, van Rensburg LJ: An aberrant vascular channel in the petrous bone: persistent lateral capital vein? Eur Radiol, 2009; 19: 2958–64
2. Ulug T, Basaran B, Minareci O, Aydin K: An unusual complication of stapes surgery: profuse bleeding from the anteriorly located sigmoid sinus. Eur Arch Otorhinolaryngol, 2004; 261: 397–99
3. Trojanowska A, Drop A, Trojanowski P et al: External and middle ear diseases: Radiological diagnosis based on clinical signs and symptoms. Insights Imaging, 2012; 3: 33–48
4. García-González U, Cavalcanti DD, Agrawal A et al: The diploic venous system: Surgical anatomy and neurosurgical implications. Neurosurg Focus, 2009; 27: E2
5. Crocker M, Nesbitt A, Rich P, Bell B: Symptomatic venous sinus thrombosis following bone wax application to emissary veins. Br J Neurosurg, 2008; 22: 798–800
6. Kaczorowska M, Furmanek MI, Klimek P, Skarżyński H. Iatrogenic internal carotid artery pseudoaneurysm as a complication of myryngotomy in 6-years-old boy. Otolaryngol Pol, 2012; 66: 368–72
7. Kumar V, Meher R, Trehan V et al: Delayed postmastoidectomy bleed from anterior tympanic artery and its management using endovascular microcoils. Am J Otolaryngol, 2012; 33: 156–58
8. Dong C, Zhao PF, Yang JG et al: Incidence of vascular anomalies and variants associated with unilateral venous pulsatile tinnitus in 242 patients based on dual-phase contrast-enhanced computed tomography. Chin Med J, 2015; 128: 581–85
9. Tomura N, Sashi R, Kobayashi M et al: Normal variations of the temporal bone on high-resolution CT: their incidence and clinical significance. Clin Radiol, 1995; 50: 144–48
10. Choi JH, Woo HY: The neglected emissary vein in mastoidectomy; Persistent petrosquamosal sinus in the laterally located sigmoid sinus. Am J Otolaryngol, 2013; 34: 255–57
11. An YH, Wee JH, Han KH, Kim YH: Two cases of petrosquamosal sinus in the temporal bone presented as perioperative finding. Laryngoscope, 2011; 121: 381–84
12. Koesling S, Kunkel P, Schul T: Vascular anomalies, sutures and small canals of the temporal bone on axial CT. Eur J Radiol, 2005; 54: 335–43
13. San Millán Ruíz D, Gailloud P, Yilmaz H et al: The petrosquamosal sinus in humans. J Anat, 2006; 209: 711–20
14. Giesemann AM, Goetz GF, Neuburger J et al: Persistent petrosquamosal sinus: High incidence in cases of complete aplasia of the semicircular canals. Radiology, 2011; 259: 825–33
15. Marsot-Dupuch K, Gayet-Delacroix M, Elmaleh-Bergès M et al: The petrosquamosal sinus: CT and MR findings of a rare emissary vein. Am J Neuroradiol, 2001; 22: 1186–93
16. Rajati M, Shahabi A, Haghir H, Afzalaghaee M: The distance of the sigmoid sinus and the middle fossa dura from the external auditory canal in chronic otitis media. Surg Radiol Anat, 2012; 35: 477–80
17. Wang CH, Shi ZP, Liu DW et al: High computed tomographic correlations between carotid canal dehiscence and high jugular bulb in the middle ear. Audiol Neurootol, 2011; 16: 106–12
18. Atilla S, Akpek S, Uslu S et al: Computed tomographic evaluation of surgically significant vascular variations related with the temporal bone. Eur J Radiol, 1995; 20: 52–56
19. Jager L, Bonell H, Liebl M et al: CT of the normal temporal bone: Comparison of multi- and single-detector row CT. Radiology, 2005; 235: 133–41
20. Woo CK, Wie CE, Park SH et al: Radiologic analysis of high jugular bulb by computed tomography. Otol Neurotol, 2012; 33: 1283–87
21. Kawano H, Tono T, Schachern PA et al: Petrous high jugular bulb: A histological study. Am J Otolaryngol, 2000; 21: 161–68

Indexed in: [Current Contents/Clinical Medicine] [SCI Expanded] [ISI Alerting System] [ISI Journals Master List] [Index Medicus/MEDLINE] [EMBASE/Excerpta Medica] [Chemical Abstracts/CAS] [Index Copernicus]